AIAA JOURNAL
Vol. 37, No. 2, February 1999

Failure of Sandwich to Laminate Tapered Composite Structures

Scott K. Kuczma* and Anthony J. Vizzini†
University of Maryland, College Park, Maryland 20742

Failure modes and load distributions in tapered, minimum-gauge composite sandwich structures were investigated. A total of 36 unidirectional graphite-epoxy/Rohacell foamcore structures were manufactured with varying taper angles and core thicknesses. The specimens were subjected to tensile, compressive, and bending loads. Experimental data were correlated with a three-dimensional finite element model developed to determine the stress and the strain state within a tapered sandwich structure. Emphasis was placed on the root of the taper, where experimental observations suggested damage initiation.

Introduction

COMPOSITE sandwich structures provide high strength-to-weight and high bending stiffness-to-weight ratios in structural components. Composite sandwich structures provide additional benefits such as the presence of two load-carrying facesheets and an increased energy absorbency and thus greater damage tolerance to impact events. Composite sandwich structures also have fewer parts and manufacturing steps than skin panels with bonded or mechanically fastened stiffeners, making them easier to manufacture than skin panels with cocured stiffeners.[1]

Core materials commonly used in composite sandwich structures include a variety of honeycomb materials, polymer foams, and low-density woods. These core materials are sealed by the outer facesheets to protect the core from exterior moisture and to allow a lip region for drilling and other mechanical facets that might otherwise crush or inhibit the core of the sandwich structure.[2]

In typical composite sandwich structures, the core is sealed with a squared upper facesheet at the edge of the sandwich core. The core is sealed by the upper facesheet as it bonds to the lower facesheet to form a monolithic laminate. In more complex composite sandwich structures, the core is ramped down (tapered) before it is sealed between the outer facesheets. The tapering of the core can arise because of the geometric necessities of a design but also can be used to adjust or improve the load transfer mechanisms between the monolithic laminate and the sandwich laminate. Figure 1 shows a schematic drawing of a tapered region commonly found on the V-22 Osprey fuselage.[2] Figure 2 illustrates the use of the laminate lip region on Boeing's Model 360 helicopter.[3] Note that the frame and longeron load-carrying spars of the helicopter structure shown are attached to the tapered sandwich structure over the monolithic laminate region. The spars are attached here and not over the sandwich core to prevent damage of the sandwich core during load transfer from the spars.

In general, experience has shown that the tapered region is the weak link in tapered sandwich structures. This prior experience, combined with the growing usage of tapered regions in composite sandwich structures and a lack of experimental data concerning the failure mechanisms in the region of the taper, indicates a need for additional research.

The objective of this research is to develop a more fundamental understanding of the behavior of thin-gauge sandwich-to-laminate tapered composite structures subjected to static loadings. Specifically, the failure modes and load transfer characteristics are examined for a variety of tapered specimens to determine the initial failure location and the reason(s) for that failure.

Received Nov. 21, 1997; revision received Sept. 18, 1998; accepted for publication Oct. 6, 1998.

*Graduate Research Assistant, Composites Research Laboratory, Department of Aerospace Engineering. Member AIAA.

†Associate Professor, Composites Research Laboratory, Department of Aerospace Engineering. Associate Fellow AIAA.

Experimental Program

An experimental study was conducted to determine the failure modes and load distributions of tapered, minimum-gauge composite sandwich structures. A total of 36 unidirectional graphite/epoxy Rohacell foamcore specimens were fabricated with varying taper angles and core thicknesses. Each upper and lower composite facesheet was composed of three unidirectional 0-deg plies of graphite/epoxy preimpregnated tape (AS4/3501-6). The unidirectional layup eliminated the occurrence of delamination while accentuating the effect of the shifting neutral axis. The facesheets were joined at the root of the taper to form a six-ply-thick laminate. No additional edge doubler plies were added. Rohacell 71WF, flight-grade foamcore material with a density of 71 kg/m^3, was used as the sandwich core for all test specimens.

Each test specimen was grouped according to the core thickness, core taper angle, and applied loading. Table 1 lists the entire test population, indicating the core thickness, the taper angle, and the sense of the applied load for each specimen, and the four loading scenarios tested are illustrated in Fig. 3. All of the test specimens were manufactured to be 38.1 mm wide.

Specimen Manufacturing

The manufacturing process began by conditioning 305-mm^2 sections of the foamcore, planed to the desired thicknesses, at 177°C for 48 h. This 48-h heat treatment increased the compressive strength of the foam from 690 to 1034 KPa at a temperature of 177°C (Ref. 4). In addition, the heat treatment shrank the foam by up to 5% by volume, thus reducing any further creep strain from occurring during the cocure with the graphite/epoxy facesheets.

Following the conditioning, a taper was cut into the foam section on a milling machine. The result was a 305-mm-wide tapered foam section of the desired longitudinal dimension. Each ply of the upper and lower facesheet was cut from a 305-mm-wide roll of graphite/epoxy preimpregnated tape. Of the six cut plies, three were combined to form a flat unidirectional laminate. Airtac spray adhesive was applied on both sides of the foam to tack down the laminate. No additional adhesive was placed between the foam and the laminates. The tapered foamcore then was positioned (centered longitudinally) on this laminate, and the remaining three unidirectional plies then were layered over the foam section.

The resulting tapered sandwich panel was vacuum bagged and cured in an autoclave using the manufacturer's recommended cure cycle, with the exception of a reduction in the prescribed autoclave pressure from 586 to 276 KPa to prevent crushing of the core. To prevent significant core crushing and core deformations from occurring in the region of the taper, no upper-surface tool was used during the cure.[5] During the cure, the epoxy flowed and served as the adhesive layer between the laminates and the core. Following the cocure, each sandwich panel was milled into 38.1-mm-wide specimens.

Table 1 Experimental matrix

Loading	Taper angle, deg	Core thickness, mm	Length D, mm	Number
Tension	30	12.7	203.2	7
	30	25.4	241.3	5
	45	12.7	203.2	5
Compression	30	25.4	247.7	5
	40	25.4	228.6	5
	45	12.7	203.2	5
Bending	45	12.7	203.2	4

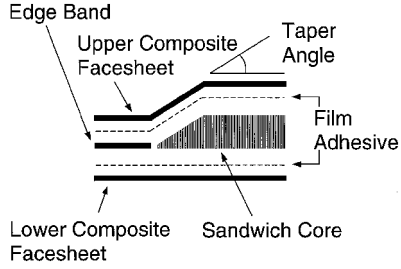

Fig. 1 Taper-region example from a V-22 Osprey fuselage.

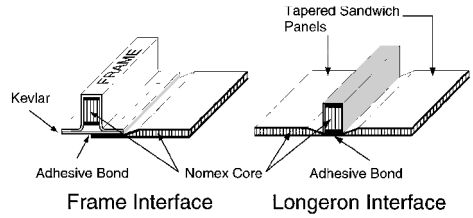

Fig. 2 Taper-region example from a Boeing Model 360 helicopter.

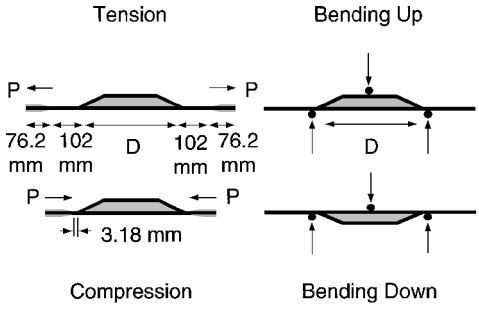

Fig. 3 Specimen manufacture dictated by load sense.

Experimental Testing and Results

All specimens were tested on a 220-kip hydraulic testing machine. Strain gauges were located at the center of the upper and lower facesheets, on the upper facesheet over the region of taper, and at a far-field section of the specimen (tension tests only). These locations were chosen to provide the necessary load transfer information from the far-field section through the region of taper and into the upper and lower facesheets. Each specimen was tested quasistatically in tension, compression, or bending under stroke control at a rate of 0.762 mm/min; load, stroke, and strain-gauge data were taken at a sampling frequency of 4 Hz. A total of 17 specimens were tested in tension, 15 in compression, and 4 in bending.

Tension

Damage resulting from loading the tapered sandwich structure in tension is shown in Fig. 4. Noticeable bending deformations (exaggerated in the figure) occurred during testing because of the asymmetrical nature of the tension specimens. Initial damage locations for all tension specimens occurred at the root of the taper originating in the resin-filled void at the tip of the tapered foamcore. However, damage propagation from this point varied between specimens with

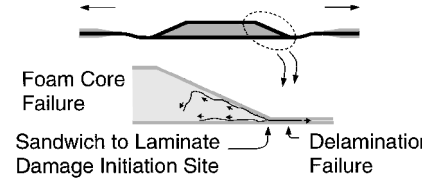

Fig. 4 Tension deformations and initial failure modes.

12.7-mm and 25.4-mm core thicknesses. The thinner specimens experienced damage propagation into the foamcore and delamination into the six-ply laminate simultaneously. The thicker specimens experienced delamination of the upper three plies and the lower three plies in the six-ply laminate region before similar damage propagation into the foamcore occurred. This difference is probably due to the relative amount of load being transferred to the upper facesheet. The thinner laminate transfers more load, which results in greater stresses in the core.

The damage propagation into the tapered region was initially observed to be debonding between the facesheets and foamcore combined with crack propagation in the resin–foamcore interface layer. The interface layer (approximately 1.0 mm thick) was formed during the cocure of the graphite/epoxy plies and the foamcore. As illustrated in Fig. 4, the original delamination event at the root of the taper propagated into the core structure along the interface layers located between the foam and the lower facesheet and the foam and the upper facesheet in the region of the taper. As damage progressed further, the crack, following the interface layer along the upper facesheet in the region of taper, kinked into the foamcore. This kinked crack propagated through the foamcore, resulting in core fracture. Eventually, this crack propagated down to the point where it intersected the already cracked interface layer located between the lower facesheet and the foamcore.

Further peeling of the upper facesheet from the core in the tapered region was observed for all tension specimens during continued loading of the lower three-ply laminate, which, at that time, carried all of the applied tensile load. Ultimate failure occurred when the longitudinal failure strength of the lower three-ply facesheet was reached.

The effect of the initial damage on the load transfer also varied among the tension specimens. In the case of the 25.4-mm-thick foamcore specimens, damage initiation caused no change in the load transfer because no load was transferred to the upper facesheet during the tensile testing. In contrast, the 12.7-mm-thick foamcore specimens exhibited a noticeable change in the load transfer following the initial damage, the reason being that the upper facesheets of the thinner specimens were carrying load at the time of the initial failure. After the initial failure, the thinner specimens lost the ability to carry load in the upper three-ply laminate because of the simultaneous delamination in the six-ply laminate and crack propagation into the core. Without this load pathway, all loading was redirected to the lower three-ply laminate.

Figures 5–7 show typical strain-gauge outputs for the three varieties of tensile specimens. In these figures, the initial damage event can be seen when the load redistributes gradually in the event of delamination (Fig. 5) or dynamically indicated by the load drop in Figs. 6 and 7. Table 2 provides averaged failure information for the tension specimens tested. Figures 5–7 illustrate the loading and failure trends observed during the testing of the tension specimens. Figure 8 is a comparison of strain output between specimens with the same 12.7-mm core thickness and varying taper angles. The strain data being compared are taken from gauges centrally located on the upper facesheets.

Figures 5–7 indicate that a thinner core aids in the transfer of more load to the upper facesheet. Figure 8 indicates that, for a given applied load, the strain in the upper facesheet of a 45-deg tapered specimen is greater than that of a 30-deg tapered specimen. For this particular case, more load is transferred as the taper angle is increased from 30 to 45 deg for equally thick specimens. In addition, the initial failure load was observed to have a stronger dependence on the core thickness than the core taper angle (see Table 2). Specimens with 25.4-mm-thick cores experienced initial failure at roughly 62%

Table 2 Failure results

Loading	Taper angle, deg	Core thickness, mm	Failure load, kN (C.V.) Initial	Ultimate
Tension	30	12.7	14.1 (4.4)	23.0 (6.3)
	30	25.4	8.8 (2.5)	20.2 (12.5)
	45	12.7	13.3 (15.7)	—[a]
Compression	30	25.4		−2.94 (12.1)
	40	25.4		−3.02 (21.4)
	45	12.7		−3.74 (10.1)

[a]Specimens not tested to ultimate failure.

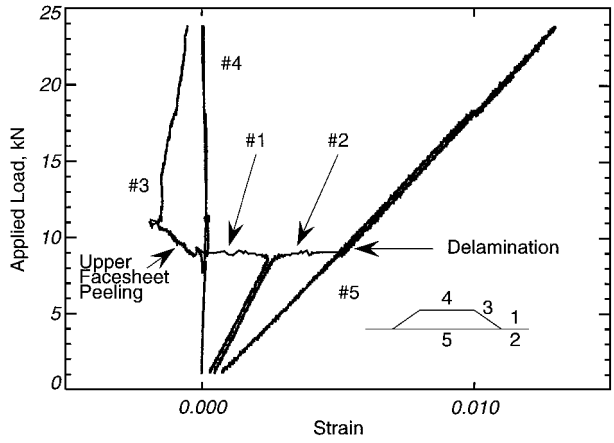

Fig. 5 Typical strain-gauge output (30-deg taper, 25.4 mm thick).

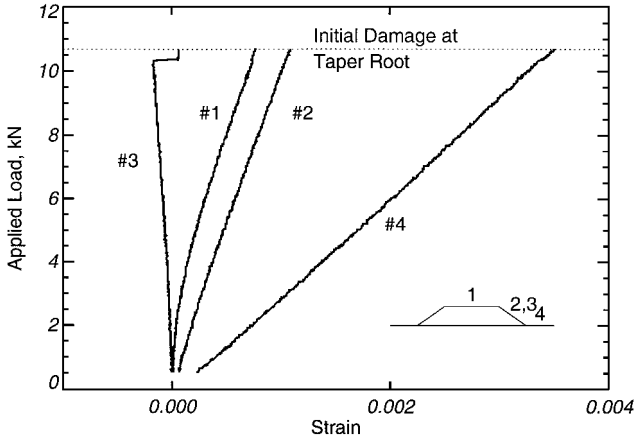

Fig. 6 Typical strain-gauge output (45-deg taper, 12.7 mm thick).

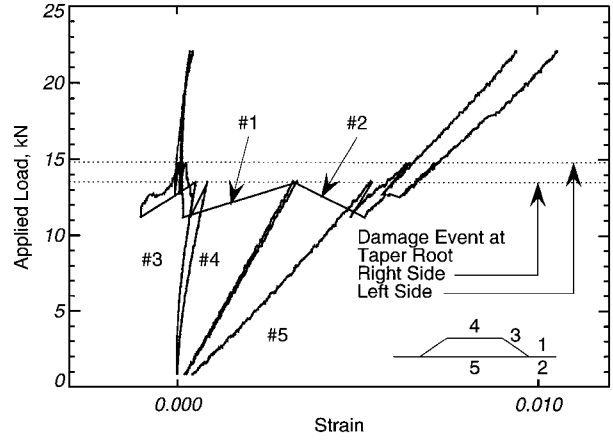

Fig. 7 Typical strain-gauge output (30-deg taper, 12.7 mm thick).

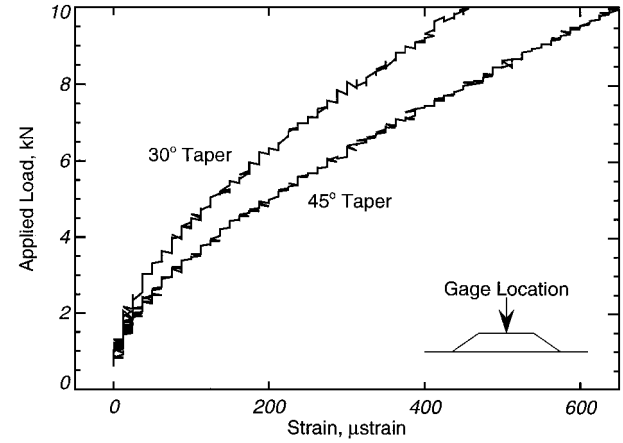

Fig. 8 Strain in upper facesheet for 30- and 45-deg specimens (12.7 mm thick).

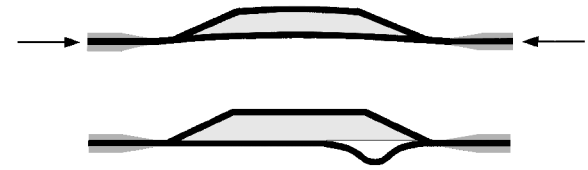

Fig. 9 Compression deformations and initial failure modes.

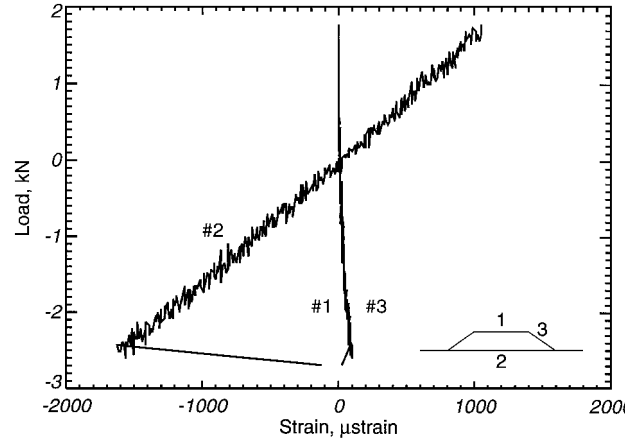

Fig. 10 Typical strain-gauge output for compression specimens.

of the initial failure load observed for specimens with 12.7-mm-thick cores.

Compression

All of the compression specimens exhibited damage in the form of lower-facesheet debonding and buckling. The lower facesheet buckled away from the core beside the root of the taper, as shown in Fig. 9, for all 15 specimens. Figure 9 also shows the noticeable bending deformations (exaggerated in the figure) that occurred during the application of a compressive load as a result of the asymmetrical nature of the specimens.

The corresponding compressive failure load did not change for the variety of taper angles. However, a small increase in failure load due to the use of a thinner core was observed experimentally. Table 2 lists the averaged failure information for the compression specimens tested, and Fig. 10 shows a representative strain-gauge output of the compressive specimens. The results show that the upper facesheet is not subjected to a compressive load. In fact, a small tensile load resulted from bending in the specimen due to its lack of symmetry. However, specimens manufactured with a 45-deg taper angle and a 12.7-mm core thickness experienced a compressive strain in the upper facesheet at lower applied load levels but changed over to a tensile strain prior to failure. Also, there was little variation in the

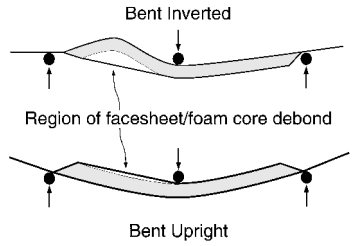

Fig. 11 Observed debonding failure for three-point bending tests.

observed failure load between the compression specimens, regardless of their geometry. No further loading was able to be transferred through the specimen after buckling of the lower facesheet.

Previous research on the debonding of foamcore sandwich panels suggests that the debonding failure mode is preceded by other failure modes, such as face yielding, face wrinkling, or core shearing, unless a sufficiently large debonded region exists between the facesheet and the core.[6] For the compression specimens tested, the observed debonding was caused by a growing delamination between the core and facesheet originating at the root of the taper.

Bending

All of the bending specimens were tested using a three-point bending test fixture. Specimens were placed in the test fixture in such a manner as to be centrally displaced from either the upper or lower facesheet. Damage in all cases took the form of the upper facesheet debonding from the foamcore. Figure 11 shows the observed deformations for the two separate bending orientations utilized. Debonding in all cases occurred near an applied loading of 500 N. As a constant rate of vertical displacement continued, further structural deformations resulted while the region of debonding grew. After the initial debonding failure, the applied loading was observed to decrease as the size of the debond grew in length.

Analytical Modeling

The three-dimensional finite element model TAPER[7] was used to determine the stress and strain within the sandwich to laminate tapered structures. In particular, the damage initiation site, the load-carrying contributions of the upper and lower facesheets, and the load transfer in the region of taper were determined.

The linear model utilizes eight-node, 24-degree-of-freedom, assumed-stress hybrid solid brick elements. The assumed material properties used are provided in Table 3 (L. Kruska, private communication, Rohm Tech, Inc.), and a representative mesh at the root of the taper is shown in Fig. 12. Because of symmetry in the longitudinal and width directions, only one-quarter of the specimen was examined. Figure 12 shows the resin layers located between the three-ply facesheets and the foamcore that meet at the root of the taper and extend into the six-ply laminate. The thickness of these layers was assumed to be 10% of the ply thickness.

Interlaminar Resin Stresses

Under an axial displacement, the interlaminar normal and shear stresses increase in magnitude near the root of the taper, as shown in Fig. 13. Three peak interlaminar stresses are indicated. Because the specimens were modeled with only one finite element through the half-width, the interlaminar shear stress σ_{yz} was neglected. These high interlaminar stresses, especially the interlaminar shear stress over a significant length, indicate that damage should initiate at the root of the taper. This observation correlates well with the experiments.

The peak interlaminar stresses as a function of the taper angle were determined for a 12.7-mm-thick core and are plotted in Fig. 14. The interlaminar shear stress is not greatly affected by the taper angle in the region examined. Indeed, between 30 and 45 deg, the interlaminar shear stress varies less than 1%. However, the interlaminar normal stress is greatly affected by the taper angle. Both the maximum compressive and tensile interlaminar normal stresses increase with increasing taper angle. For the 12.7-mm-thick specimens tested in tension with taper angles of 30 and 45 deg, the percentage increases in the interlaminar normal and shear stresses are 53% and 1.4%, respectively. However, the difference in failure

Table 3 Material properties

Material	Property
AS4/3501-6 graphite/epoxy	
Longitudinal modulus	$E_L = 147.5$ GPa
Transverse modulus	$E_T = 9.65$ GPa
In-plane shear modulus	$G_{LT} = 6.84$ GPa
Out-of-plane shear modulus	$G_{TN} = 5.5$ GPa
Major Poisson's ratio	$\nu_{LT} = 0.30$
Out-of-plane Poisson's ratio	$\nu_{TN} = 0.54$
Ply thickness	$t_{\text{ply}} = 0.134$ mm
Rohacell 71 WF[a]	
Young's modulus	$E = 137.9$ MPa
Shear modulus	$G = 27.6$ MPa
Poisson's ratio	$\nu = 0.30$
Neat resin	
Young's modulus	$E = 3.93$ GPa
Poisson's ratio	$\nu = 0.37$

[a]Kruska, private communication.

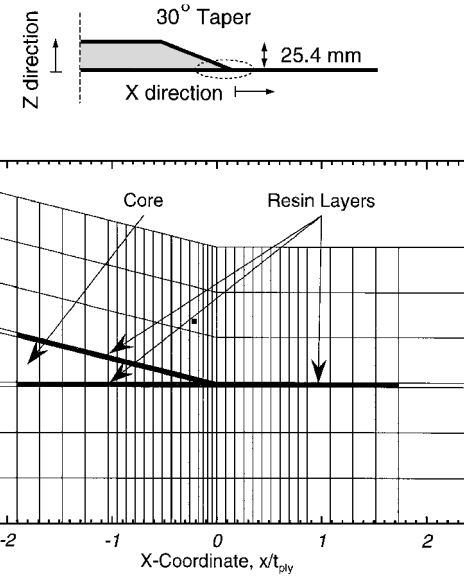

Fig. 12 Finite element model.

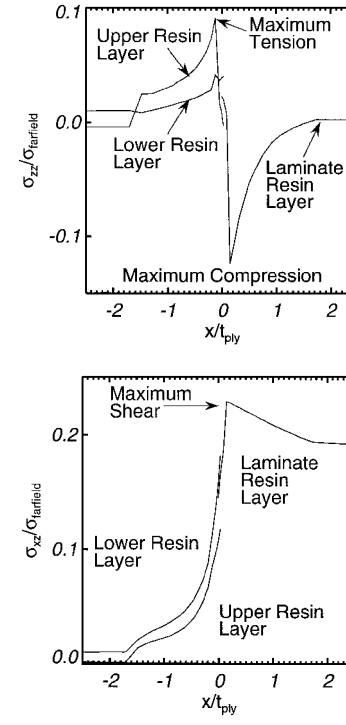

Fig. 13 Interlaminar stresses at taper root.

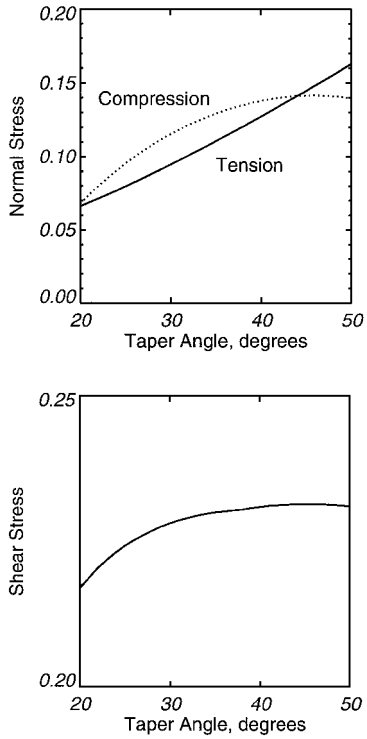

Fig. 14 Maximum interlaminar stresses at taper root (12.7 mm thick).

load decreased by only 5.7%. For the 25.4-mm-thick specimens tested in compression with taper angles of 30 and 40 deg, the percentage increases in the interlaminar normal and shear stresses are 19% and 1.9%, respectively. However, the difference in failure load increased by 2.7%. This indicates that the damage mechanism is not dominated by the interlaminar normal stresses but is likely to be controlled by the magnitude, and the gradient, of the interlaminar shear stress at the taper root.

Load Transfer

The degree of linearity of the elastic response in different regions of the specimens can be determined by observing the ratio of strains. In compression the strain in the top facesheet is proportional to the strain in the bottom facesheet when the core thickness is 25.4 mm for both the 30- and 40-deg tapers. For the thin-core (12.7-mm) specimens, proportionally less load is transferred to the top facesheet as the load is increased, in part because of the reduced bending stiffness of the specimen. In general, the finite element model predicts the top-surface strain levels, considering that less than 5% of the load is transferred.

Tension comparisons between the model and experiment in the upper and lower facesheets at the center of the specimen indicate that the initial experimental data and model output are in agreement. However, as the loading increases, the experimental data and model prediction begin to differ significantly. This lack of agreement is a result of the nonlinear deformations that occurred in the specimen due to the out-of-plane bending that resulted from the lack of symmetry in the structure. This bending caused the amount of load carried by the upper facesheet to increase as the overall load applied to the specimen increased; this was not predicted analytically.

The model also was used to predict the amount of curvature at the center of the thick section for each of the different specimen geometries. The predicted curvature results were compared with the experimentally recorded curvature values. The model and experiment agree initially, for example, up to 5 kN for the 30-deg taper, 12.7-mm-thick specimens. Above this point the applied load is proportional to the measured curvature; however, the slope indicates that the specimen has stiffened. In general, the model was able to predict the initial proportionality of the load to the curvature.

Conclusions

A total of 36 tapered sandwich-to-laminate specimens were tested in tension, compression, and bending. The resultant failure modes, failure loads, and load-carrying aspects of each structure were investigated. Analytically, the interlaminar resin stresses and the load transfer were determined and correlated with the experimental observations.

The tensile tests indicate that the initial damage occurs at the root of taper and the propagation of damage is dependent on core thickness. A thinner core results in a higher initial failure load and more load transfer to the upper facesheet. Load transfer was more dependent on the core thickness than the taper angle.

The compression tests also indicate that the initial damage occurs at the root of the taper; however, damage propagation is independent of core thickness and taper angle. All specimens experienced similar failure modes and damage propagation into the core. Damage initiating at the taper root takes the form of delamination growth into the interface layer between the core and the lower facesheet. As the delamination or crack length reaches a critical length, the lower facesheet buckles away from the core section.

The compression data suggest that the initial failure load is not sensitive to the taper angle in the range tested. However, the data clearly indicate that the thickness of the specimen greatly affects the initial failure load. The failure load decreased by 20% with an increase of core thickness from 12.7 to 25.4 mm.

In general, core thickness and taper angle both affect the load transfer into the upper facesheet, although it is the thickness that has the greatest effect on the initiation of damage. The taper angle does not appreciably change the interlaminar shear stress at the taper root, which appears to be the governing stress in the initial failure. Thus, the design of the sandwich structures must properly account for the shifting of the neutral axis due to thickness.

Linear analysis of such a tapered sandwich structure appears to be inadequate. Small deflections on the order of the facesheet thickness occur as a result of the shifting of the neutral axis. These deflections result in geometric nonlinearities that greatly limit the application of linear stress analyses.

References

[1] Weems, D., and Llorente, S. G., "Evaluation of a Simplified Approach to In-Plane Shear Testing for Damage Tolerance Evaluation," *Proceedings of the American Helicopter Society 46th Annual Forum*, Washington, DC, 1990, pp. 713–720.

[2] Schulze, E. J., and Kesack, W. J., "Honeycomb Sandwich Composite Structures Used on the V-22 Osprey Fuselage," *Proceedings of the 22nd International SAMPE Technical Conference*, Vol. 22, Boston, MA, 1990, pp. 1051–1069.

[3] Llorente, S., "Honeycomb Sandwich Primary Structure Applications on the Boeing Model 360 Helicopter," *Proceedings of the 34th International SAMPE Symposium*, Vol. 34, Book 1, Reno, NV, 1989, pp. 824–838.

[4] Atanasoff, H., and Vizzini, A. J., "Foam Tool Manufacture of Stiffness-Coupled Composite Box Beams," *SAMPE Quarterly*, Vol. 23, No. 3, 1992, pp. 37–42.

[5] Llorente, S., Fay, R., and Kitson, L., "Strength and Damage Tolerance Evaluation of Sandwich Structure Manufactured Utilizing the Automated Tow-Placement Process," *Proceedings of the American Helicopter Society 49th Annual Forum*, St. Louis, MO, 1993, pp. 115–124.

[6] Triantafillou, T. C., and Gibson, L. J., "Debonding in Foam-Core Sandwich Panels," *Materials and Structures*, Vol. 22, 1989, pp. 64–69.

[7] Vizzini, A. J., and Lee, S. W., "Damage Analysis of Composite Tapered Beams," *Journal of the American Helicopter Society*, Vol. 40, No. 2, 1995, pp. 43–49.

A. M. Waas
Associate Editor